





Article

Derivation of Meson Masses in SU(3) and SU(4) Extended Linear Sigma Model at Finite Temperature

Abdel Nasser Tawfik ^{1,*}, Azar I. Ahmadov ², Alexandra Friesen ³, Yuriy Kalinovsky ³, Alexey Aparin ³
and Mahmoud Hanafy ⁴

¹ Basic Science Department, Faculty of Engineering, Future University in Egypt, New Cairo 11835, Egypt

² Institute for Physical Problems, Baku State University, Z. Khalilov St. 23, AZ1148 Baku, Azerbaijan

³ Joint Institute for Nuclear Research (JINR), 141980 Dubna, Russia

⁴ Physics Department, Faculty of Science, Benha University, Benha 13518, Egypt

* Correspondence: a.tawfik@fue.edu.eg

Abstract: The present study focused on the mesonic potential contributions to the Lagrangian of the extended linear sigma model (eLSM) for scalar and pseudoscalar meson fields across various quark flavors. The present study focused on the low-energy phenomenology associated with quantum chromodynamics (QCD), where mesons and their interactions serve as the pertinent degrees of freedom, rather than the fundamental constituents of quarks and gluons. Given that SU(4) configurations are completely based on SU(3) configurations, the possible relationships between meson states in SU(3) and those in SU(4) were explored at finite temperature. Meson states, which are defined by distinct chiral properties, were grouped according to their orbital angular momentum J , parity P , and charge conjugation C . Consequently, this organization yielded scalar mesons with quantum numbers $J^{PC} = 0^{++}$, pseudoscalar mesons with $J^{PC} = 0^{-+}$, vector mesons with $J^{PC} = 1^{-}$, and axial vector mesons with $J^{PC} = 1^{++}$. We accomplished the derivation of analytical expressions for a total of seventeen noncharmed meson states and twenty-nine charmed meson states so that an analytical comparison of the noncharmed and charmed meson states at different temperatures became feasible and the SU(3) and SU(4) configurations could be analytically estimated.



Academic Editor: Maxim Yu. Khlopov

Received: 31 December 2024

Revised: 17 January 2025

Accepted: 20 January 2025

Published: 22 January 2025

Citation: Tawfik, A.; Ahmadov, A.I.; Friesen, A.; Kalinovsky, Y.; Aparin, A.; Hanafy, M. Derivation of Meson Masses in SU(3) and SU(4) Extended Linear Sigma Model at Finite Temperature. *Particles* **2025**, *8*, 9. <https://doi.org/10.3390/particles8010009>

Copyright: © 2025 by the authors. Licensee MDPI, Basel, Switzerland. This article is an open access article distributed under the terms and conditions of the Creative Commons Attribution (CC BY) license (<https://creativecommons.org/licenses/by/4.0/>).

Keywords: chiral Lagrangian; sigma model; charmed mesons; effective QCD models

1. Introduction

Perturbative approaches to quantum chromodynamics (QCD) yield effective solutions, particularly at very high energy scales [1]. In contrast, nonperturbative solutions require numerical methods for their approximation [2]. The substantial computational costs associated with these methods highlight the necessity for accurate solutions at nonzero density. Nevertheless, numerical lattice QCD simulations face limitations at a finite density, known as the “sign problem” [3]. This situation has led to the adoption of effective models [4,5], such as the hadron resonance gas model [6–9]. As for QCD-like effective models, the Nambu–Jona–Lasinio (NJL) model appears as a widely used approach [10–12] that was introduced to investigate the source of the nucleon mass as a self-energy within a framework characterized by four-fermion interactions, drawing parallels with the emergence of an energy gap in superconductivity theory [13]. This model serves as a phenomenological representation of quarks, exhibiting chiral symmetry breaking at low densities and temperatures, while restoring chiral symmetry at elevated densities and temperatures. In the phase where chiral symmetry is broken, quarks acquire a dynamical mass through their

interactions with the vacuum. Furthermore, QCD-like models, including the extended linear sigma model (eLSM) introduced in the 1960s, are significant due to their shared global symmetries with QCD and their lower computational requirements [14–17]. In this context, it is important to note that the Lagrangian associated with the gauge theory governing the color interactions of quarks and gluons exhibits invariance under local color transformations. This property ensures that the physical implications remain unchanged when the colors of quarks and gluons undergo transformation. Conversely, the interactions themselves do not depend on the flavor. In the effective QCD eLSM, the global chiral symmetry is explicitly broken due to the presence of nonzero quark masses and quantum effects, as discussed in the literature [18]. Additionally, this symmetry is spontaneously broken by the nonzero expectation value of the quark condensate within the QCD vacuum.

The eLSM is utilized when exploring various QCD symmetries. This includes (i) isospin symmetry, which is characterized as a global transformation linked to SU(2) rotations in the flavor space of up and down quarks, where the Lagrangian remains invariant for equal or negligible masses [19–21]. Moreover, (ii) global chiral symmetry is maintained in the chiral limit of massless QCD, where left- and right-handed components exhibit symmetry. Nonetheless, this symmetry is violated due to the properties of the QCD vacuum, including the Higgs mechanism, which leads to pions being recognized as the lightest Goldstone bosons resulting from the broken symmetry [22,23]. The eLSM investigation also addresses (iii) discrete symmetries, such as charge conjugation (C), parity (P), and time reversal (T) [24], along with (iv) classical dilatation (scale) symmetry [25].

Before the establishment of QCD, which serves as the theoretical foundation for strong interactions, Gell–Mann and Levy proposed the sigma model to introduce a field associated with a point particle. This field is restricted to a defined manifold and characterizes the interactions of pions [26]. The field corresponds to a spinless sigma, referred to as the scalar meson. A variety of studies utilized the LSM, including the $\mathcal{O}(4)$ LSM [26]. The implementation of the LSM, which incorporates quark degrees of freedom, is enabled by an extension that realizes the dynamic nature of pseudoscalar and scalar mesons as a linear representation of chiral symmetry, which experiences weak breaking due to the current quark masses. This study was dedicated to exploring the low-energy phenomenology of quantum chromodynamics (QCD) [27], emphasizing mesons and their interactions as the relevant degrees of freedom, in contrast to the fundamental elements of quarks and gluons. Thus, the model can be regarded as an effective representation of nonperturbative QCD [28–32] that helps in understanding the emergence of hadron masses and structures [33].

Chiral symmetry is commonly viewed as a foundational approximation for understanding the structure of hadrons. Approximately forty years ago, calculations of the spin-zero mass spectrum and leptonic decay constants were performed using the one-loop approximation of the SU(4) linear sigma model [32]. The extended linear sigma model (eLSM) investigates the phenomenological aspects of charmed mesons [24]. More recently, the quark–hadron phase diagram was examined at constrained temperatures and densities through the mean-field approximation of the SU(4) Polyakov linear sigma model (PLSM) [34,35]. It was proposed that the $N_f = 4$ Lagrangian bears similarities to the $N_f = 3$ Lagrangian. In a thorough investigation, one of the contributing authors, A.T., utilized the SU(3) PLSM to analyze the thermodynamic behavior, phase structure, and meson masses of QCD across a range of finite temperatures, densities, and magnetic fields. This extensive research [19,36–45] provided critical insights into various fundamental features of QCD.

The present study utilized an eLSM that featured two configurations. The first configuration included three flavors of quarks, while the second configuration incorporated an additional charm quark flavor. Each configuration was combined with scalar and pseudoscalar meson fields [34,35,46,47]. To simplify our discussion, we analyzed the contri-

butions of each configuration to the meson potential. The quark sets enabled an analytical evaluation of various meson states, expressed as $\langle \bar{q}q \rangle = \langle \bar{q}_\ell q_r - \bar{q}_\ell q_r \rangle \neq 0$ [48]. Meson states, which exhibit distinct chiral structures, were organized according to certain quantum numbers, including the orbital angular momentum J , parity P , and charge conjugation C . This organization resulted in the classification of scalar mesons as $J^{PC} = 0^{++}$, pseudoscalar mesons as $J^{PC} = 0^{-+}$, vector mesons as $J^{PC} = 1^{--}$, and axial vector mesons as $J^{PC} = 1^{++}$ [37,43]. We compiled analytical results for seventeen noncharmed meson states and twenty-nine charmed meson states at finite temperature. The focus of this study was to undertake an analytical comparison of the noncharmed and charmed meson states at different temperatures. The analysis of density dependence could be addressed in a separate manuscript. The fundamental argument suggests that density should be depicted in a manner comparable with that of temperature.

This manuscript is structured in the following manner: Section 2 introduces the underlying formalism. The details of the SU(3) configuration and the seventeen noncharmed meson states are provided in Section 2.1. Section 2.2 presents the SU(4) configuration, along with the twenty-nine charmed meson states. Lastly, Section 3 is devoted to the conclusions and an outlook on future research.

2. Mesonic Potential of Extended Linear Sigma Model

The sigma model integrates chiral symmetry through a linear representation [26]. Unlike the nonlinear representation, which addresses only the Goldstone bosons and omits vector mesons, the linear representation permits a comprehensive study of both Goldstone bosons and scalar mesons. This expansion into the vector sector allows for the inclusion of vector and axial vector mesons. The eLSM acknowledges chiral symmetry in conjunction with other QCD symmetries [49]. In Section 2.1, we introduce the SU(3) mesonic potential. Comprehensive information regarding the complete Lagrangian is available in Ref. [50]. Amendments to specific expressions found in Ref. [50] are detailed in the Appendix A. Moreover, we introduce an analytical description for seventeen meson states, expanding our discussion to encompass finite-temperature considerations. This analysis aimed to assess the influence of finite temperature on the analytical expressions related to meson states.

2.1. SU(3) Configuration

Let us start by introducing the SU(3) mesonic potential:

$$\begin{aligned}
 U(\sigma_x, \sigma_y) &= \frac{m^2}{2} (\sigma_x^2 + \sigma_y^2) - \frac{c}{2\sqrt{2}} \sigma_x^2 \sigma_y + \frac{\ell_1}{2} \sigma_x^2 \sigma_y^2 + \frac{1}{8} (2\ell_1 + \ell_2) \sigma_x^4 \\
 &+ \frac{1}{4} (\ell_1 + \ell_2) \sigma_y^4 - h_x \sigma_x - h_y \sigma_y.
 \end{aligned} \tag{1}$$

The minimal global minimization of the grand potential allows for the deduction of the light quark condensates, denoted as σ_x and σ_y , which represent the light and strange quark condensates, respectively.

All condensates and parameters in the effective mesonic potential equation (Equation (1)) shall be regarded as functions of temperature. The temperature dependence of T , m , h_x , and h_y are explicitly given in (2), (3), (5), and (6), respectively. To examine the temperature dependence of the various quantities associated with eLSM, we begin with

$$m^2(T) = m^2 \left(1 - \frac{T^2}{T_0^2} \right), \quad \text{where } T_0 \simeq \Lambda_{\text{QCD}}, \quad (2)$$

$$T_{N_c}(T) = \frac{T_0}{\sqrt{1 + \frac{T^2}{2f_\pi^2} \frac{3}{N_c}}}, \quad \text{where } \lim_{N_c \rightarrow \infty} T_{N_c} = T_0, \quad (3)$$

where T_0 is the deconfinement critical temperature [22,39,51] and N_c refers to the color degrees of freedom found in non-Abelian $SU(N_c)$ gauge theory [52]. Additionally, $T_{N_c}(T)$ is the critical temperature that characterizes gauge QCD, which includes color degrees of freedom, and Λ_{QCD} denotes the energy scale associated with QCD [53].

The anomaly-breaking term \mathcal{C} associated with $U(1)_A$ is constrained by the function $\ell_2(T)$, alongside the mass difference observed between pions and kaons:

$$\mathcal{C}(T) = \frac{m_K^2(T) - m_\pi^2(T)}{f_K - f_\pi} - \ell_2(2f_K - f_\pi). \quad (4)$$

Under the conditions where $\frac{\partial U}{\partial \sigma_x} = 0$ and $\frac{\partial U}{\partial \sigma_y} = 0$, the quantities $h_x(T)$ and $h_y(T)$ can be analytically determined:

$$h_x(T) = m^2(T)\sigma_x(T) - \frac{\mathcal{C}}{\sqrt{2}}\sigma_x(T)\sigma_y(T) - \ell_1(T)\sigma_x(T)\sigma_y^2(T) + \frac{1}{2}[2\ell_1(T) + \ell_2(T)]\sigma_x^3(T), \quad (5)$$

$$h_y(T) = m^2(T)\sigma_x(T) - \frac{\mathcal{C}}{2\sqrt{2}}\sigma_x^2(T) - \ell_1(T)\sigma_x^2(T)\sigma_y(T) + [\ell_1(T) + \ell_2(T)]\sigma_y^3(T). \quad (6)$$

The dependence of ℓ_1 and ℓ_2 on temperature is represented as follows:

$$\ell_1(T) = \frac{m_\sigma^2(T) - m_\pi^2(T) - m_{a_0}^2(T) + m_\eta^2(T)}{3f_\pi^2}, \quad (7)$$

$$\ell_2(T) = \frac{3[2f_K - f_\pi]m_K^2(T) - 3[2f_K - f_\pi]m_\pi^2(T) - 2[f_K - f_\pi][m_{\eta'}^2(T) + m_\eta^2(T)]}{[f_K - f_\pi][3f_\pi^2 + 8f_K(f_K - f_\pi)]}, \quad (8)$$

where f_π is the pion decay constant [54] and f_K is the kaon decay constant [55]. Moreover, within this configuration, the masses corresponding to the meson states, namely, $m_\pi(T)$, $m_K(T)$, $m_\sigma(T)$, $m_{a_0}(T)$, $m_\eta(T)$, and $m_{\eta'}(T)$, were calculated.

Now, the formulation of analytical expressions regarding the masses of seventeen noncharmed mesons, emphasizing their relationship with finite temperatures, shall be outlined. The grand potential can be derived in the mean field approximation. Given the assumption of thermal equilibrium, the grand partition function is expressed via a path integral that includes the quark, antiquark, and meson fields:

$$\mathcal{Z} = \text{Tr} \exp[-\hat{\mathcal{H}}/T] = \int \prod_a \mathcal{D}\sigma_a \mathcal{D}\pi_a \int \mathcal{D}\psi \mathcal{D}\bar{\psi} \exp \left[\int_x \mathcal{L} \right], \quad (9)$$

where $\int_x \equiv i \int_0^{1/T} dt \int_V d^3x$, and t is the time for which the system with volume V evolves. The present analysis assumed a vanishing density, which corresponds to a vanishing chemical potential. The partition function can be derived using the mean field approximation [56–58]. In this context, the meson fields are substituted with their expectation values, specifically $\bar{\sigma}_x$ and $\bar{\sigma}_y$, within the action [59,60]. By employing standard techniques [60], we can perform the integration over the fermionic contributions, leading to the derivation of the effective potential for the mesons:

$$\Omega(T) = \frac{-T \ln \mathcal{Z}}{V} = U(\sigma_x, \sigma_y) + \mathcal{U}(\Phi, \Phi^*, T) + \Omega_{\bar{\psi}\psi}, \tag{10}$$

where the fields Φ and Φ^* are defined (Equation (38)) as a complex matrix of dimensions $N_f \times N_f$, which includes the scalar σ_a with quantum numbers $J^{PC} = 0^{++}$, pseudoscalar π_a with $J^{PC} = 0^{-+}$, vector mesons that possess $J^{PC} = 0^{-+}$, and axial vector mesons that share the quantum numbers $J^{PC} = 0^{++}$. The mesonic potential is explicitly elaborated herein. Additional information on the other potentials $\mathcal{U}(\Phi, \Phi^*, T)$ and $\Omega_{\bar{\psi}\psi}$ can be found in previously published works [19,36–45].

By taking the second derivative of the grand potential evaluated at its minimum with respect to the corresponding fields, the masses of various states can be obtained. In the present calculations, the minima were estimated by vanishing expectation values of all the scalar, pseudoscalar, vector, and axial vector fields:

$$m_{i,ab}^2 = \left. \frac{\partial^2 \Omega(T)}{\partial \beta_{i,a} \partial \beta_{i,b}} \right|_{\min}, \tag{11}$$

where $\beta_{i,a}$ and $\beta_{i,b}$ are the corresponding mass fields of the i -th hadron state. $a, b \in [0, 1, \dots, 8]$.

- Scalar noncharmed mesons:

$$m_{\sigma_N}^2(T) = m_0^2 \left(1 - \frac{T^2}{T_0^2} \right) + \frac{3}{2} \ell_2(T) \sigma_x^2(T), \tag{12}$$

$$m_{K_0^*}^2(T) = Z_{K_0^*}^2(T) \left[m_0^2 \left(1 - \frac{T^2}{T_0^2} \right) + \frac{\ell_2(T)}{2} \sigma_x^2(T) + \frac{\ell_2(T)}{\sqrt{2}} \sigma_x(T) \sigma_y(T) + \ell_2(T) \sigma_y^2(T) \right], \tag{13}$$

$$m_{a_0}^2(T) = m_0^2 \left(1 - \frac{T^2}{T_0^2} \right) + \frac{3}{2} \ell_2(T) \sigma_x^2(T), \tag{14}$$

$$m_{\sigma_S}^2(T) = m_0^2 \left(1 - \frac{T^2}{T_0^2} \right) + 3 \ell_2(T) \sigma_y^2(T). \tag{15}$$

- Pseudoscalar noncharmed mesons:

$$m_{\pi}^2(T) = Z_{\pi}^2(T) \left[m_0^2 \left(1 - \frac{T^2}{T_0^2} \right) + \frac{\ell_2(T)}{2} \sigma_x^2(T) \right], \tag{16}$$

$$m_K^2(T) = Z_K^2(T) \left[m_0^2 \left(1 - \frac{T^2}{T_0^2} \right) + \frac{\ell_2(T)}{2} \sigma_x^2(T) - \frac{\ell_2(T)}{\sqrt{2}} \sigma_x(T) \sigma_y(T) + \ell_2(T) \sigma_y^2(T) \right], \tag{17}$$

$$m_{\eta_N}^2(T) = Z_{\eta_N}^2(T) \left[m_0^2 \left(1 - \frac{T^2}{T_0^2} \right) + \frac{\ell_2(T)}{2} \sigma_x^2(T) + \mathcal{D} \sigma_x^2(T) \sigma_y^2(T) \right], \tag{18}$$

$$m_{\eta_S}^2(T) = Z_{\eta_S}^2(T) \left[m_0^2 \left(1 - \frac{T^2}{T_0^2} \right) + \ell_2(T) \sigma_y^2(T) + \frac{\mathcal{D}}{4} \sigma_x^4(T) \right], \tag{19}$$

$$m_{\eta_{NS}}^2(T) = Z_{\pi}(T) Z_{\pi_3}(T) \frac{\mathcal{D}}{2} \sigma_x^3(T) \sigma_y(T). \tag{20}$$

- Axial vector noncharmed mesons:

$$m_{a_1}^2(T) = m_1^2(T) - m_0^2 \frac{T^2}{T_0^2} + \frac{1}{2} (2g_1^2(T) + h_2(T) - h_3(T)) \sigma_x^2(T), \quad (21)$$

$$m_{K_1}^2(T) = m_1^2(T) - m_0^2 \frac{T^2}{T_0^2} + \frac{1}{4} (g_1^2(T) + h_2(T)) \sigma_x^2(T) - \frac{1}{\sqrt{2}} \sigma_x(T) \sigma_y (h_3(T) - g_1^2(T)) + \frac{1}{2} (h_2(T) + g_1^2(T)) \sigma_y^2(T) + \delta_s(T), \quad (22)$$

$$m_{f_{1s}}^2(T) = m_1^2(T) - m_0^2 \frac{T^2}{T_0^2} + (2g_1^2(T) + h_2(T) - h_3(T)) \sigma_y^2(T) + 2\delta_s(T), \quad (23)$$

$$m_{f_{1N}}^2(T) = m_{a_1}^2(T). \quad (24)$$

- Vector noncharmed mesons:

$$m_\rho^2(T) = m_1^2(T) - m_0^2 \frac{T^2}{T_0^2} + \frac{1}{2} (h_2(T) + h_3(T)) \sigma_x^2(T), \quad (25)$$

$$m_{K^*}^2(T) = m_1^2(T) - m_0^2 \frac{T^2}{T_0^2} + \frac{1}{4} (g_1^2(T) + h_2(T)) \sigma_x^2(T) + \frac{1}{\sqrt{2}} \sigma_x(T) \sigma_y (h_3(T) - g_1^2(T)) + \frac{1}{2} (h_2(T) + g_1^2(T)) \sigma_y^2(T) + \delta_s(T), \quad (26)$$

$$m_{\omega_s}^2(T) = m_1^2(T) - m_0^2 \frac{T^2}{T_0^2} + (h_2(T) + h_3(T)) \sigma_y^2(T) + 2\delta_s(T), \quad (27)$$

$$m_{\omega_N}^2(T) = m_\rho^2(T). \quad (28)$$

The different quantities present in the mass expressions are outlined as follows:

$$g_1^2(T) = \frac{m_{a_1}^2(T)}{f_\pi^2 Z_\pi^2} \left(1 - \frac{1}{Z_\pi^2} \right), \quad (29)$$

$$\mathcal{D}(T) = \frac{1}{2} (m_\eta^2(T) - m_\pi^2(T)), \quad (30)$$

$$\delta_s(T) = \frac{1}{2} \left\{ m_{\omega_s}^2(T) - m_1^2(T) + m_0^2 \frac{T^2}{T_0^2} - \left[\frac{h_1^2(T)}{2} + h_2(T) + h_3(T) \right] \sigma_y^2(T) - \frac{h_1(T)}{2} \sigma_x^2(T) \right\}, \quad (31)$$

$$m_1^2(T) = m_{\omega_s}^2(T) - \left[\frac{h_1(T)}{2} + h_2(T) - h_3(T) \right] \sigma_s^2(T) - \frac{h_1(T)}{2} \sigma_s(T) - 2\delta_s(T), \quad (32)$$

$$Z_\pi(T) = Z_{\eta_N}(T) = \frac{m_{a_1}(T)}{\sqrt{m_{a_1}^2(T) - g_1^2(T) \sigma_x^2(T)}}, \quad (33)$$

$$Z_K(T) = \frac{2m_{K_1}(T)}{4m_{K_1}^2(T) - g_1^2(T) [\sigma_x(T) + \sqrt{2}\sigma_y(T)]^2}, \quad (34)$$

$$Z_{\eta_s}(T) = \frac{m_{f_{1s}}(T)}{m_{f_{1s}}^2(T) - 2g_1^2(T) \sigma_y^2(T)}, \quad (35)$$

$$Z_{K_0^*}(T) = \frac{2m_{K_0^*}(T)}{4m_{K_0^*}^2(T) - g_1^2(T) [\sigma_x(T) - \sqrt{2}\sigma_y(T)]^2}. \quad (36)$$

Section 2.2 introduces further analytical representations of meson states. This discussion specifically emphasizes the charmed meson states, which exhibit variations in response to changes in temperature.

2.2. SU(4) Configuration

It is assumed that the Lagrangian for $N_f = 4$, which maintains global chiral invariance [34], is similar to that of $N_f = 3$ [61]. In the context of $N_f = 4$, the mass term $-2 \text{Tr}[\epsilon \Phi^\dagger \Phi]$ must be integrated into the eLSM Lagrangian [18]. The corresponding mesonic grand potential is given as

$$\begin{aligned}
 U_m^{SU(4)}(\Phi) = & \frac{m^2}{2} (\sigma_x^2 + \sigma_y^2 + \sigma_{15}^2) + \ell_1 \left[4 \left(\sigma_x + \frac{\sigma_{15}}{\sqrt{6}} \right)^4 + \left(\sqrt{2}\sigma_y + \frac{\sigma_{15}}{\sqrt{6}} \right)^4 \right. \\
 & + \left(\sqrt{\frac{2}{3}}\sigma_0 - \sqrt{\frac{3}{2}}\sigma_{15} \right)^4 + 4 \left(\sigma_x + \frac{\sigma_{15}}{\sqrt{6}} \right)^2 \left(\sqrt{2}\sigma_y + \frac{\sigma_{15}}{\sqrt{6}} \right)^2 \\
 & \left. + 4 \left(\sigma_x + \frac{\sigma_{15}}{\sqrt{6}} \right)^2 \left(\sqrt{\frac{3}{2}}\sigma_0 - \sqrt{\frac{3}{2}}\sigma_{15} \right)^2 + 2 \left(\sqrt{2}\sigma_y + \frac{\sigma_{15}}{\sqrt{6}} \right)^2 \left(\sqrt{\frac{2}{3}}\sigma_0 - \sqrt{\frac{3}{2}}\sigma_{15} \right)^2 \right] \\
 & + \ell_2 \left[2 \left(\sigma_x + \frac{\sigma_{15}}{\sqrt{6}} \right)^4 + \left(\sqrt{2}\sigma_y + \frac{\sigma_{15}}{\sqrt{6}} \right)^4 + \left(\sqrt{\frac{2}{3}}\sigma_0 - \sqrt{\frac{3}{2}}\sigma_{15} \right)^4 \right] \\
 & - \frac{c}{8} \left[\frac{2}{3} \sigma_x^2 \sigma_y \sigma_0 + \frac{\sigma_y \sigma_{15}^2 \sigma_0}{3\sqrt{3}} + \frac{2\sqrt{2}}{3} \sigma_x \sigma_y \sigma_{15} \sigma_0 + \frac{1}{3} \sigma_x^2 \sigma_{15} \sigma_0 + \frac{\sigma_{15}^3 \sigma_0}{8} \right. \\
 & \left. + \frac{\sqrt{2} \sigma_x \sigma_{15} \sigma_0^2}{3\sqrt{3}} - \sqrt{3} \sigma_x^2 \sigma_y \sigma_{15} - \frac{\sigma_{15}^3 \sigma_y}{2\sqrt{3}} - \sqrt{2} \sigma_x \sigma_y \sigma_{15}^2 - \frac{\sigma_x^2 \sigma_{15}^2}{2} - \frac{\sigma_{15}^4}{12} - \frac{\sigma_x \sigma_{15}^3}{\sqrt{6}} \right]. \tag{37}
 \end{aligned}$$

The field Φ is given as

$$\Phi = \sum_{a=0}^{N_f^2-1} T_a (\sigma_a + i\pi_a), \tag{38}$$

where the scalar mesons are given as

$$T_a \sigma_a = \frac{1}{\sqrt{2}} \begin{pmatrix} \frac{\sigma_0}{2} + \frac{\sigma_3}{\sqrt{2}} + \frac{\sigma_8}{\sqrt{6}} + \frac{\sigma_{15}}{2\sqrt{3}} & \frac{\sigma_1 - i\sigma_2}{\sqrt{2}} & \frac{\sigma_4 - i\sigma_5}{\sqrt{2}} & \frac{\sigma_9 - i\sigma_{10}}{\sqrt{2}} \\ \frac{\sigma_1 + i\sigma_2}{\sqrt{2}} & \frac{\sigma_0}{\sqrt{2}} - \frac{\sigma_3}{\sqrt{2}} + \frac{\sigma_8}{\sqrt{6}} + \frac{\sigma_{15}}{2\sqrt{3}} & \frac{\sigma_6 - i\sigma_7}{\sqrt{2}} & \frac{\sigma_{11} - i\sigma_{12}}{\sqrt{2}} \\ \frac{\sigma_4 + i\sigma_5}{\sqrt{2}} & \frac{\sigma_6 + i\sigma_7}{\sqrt{2}} & \frac{\sigma_0}{2} - \sqrt{\frac{2}{3}}\sigma_8 + \frac{\sigma_{15}}{2\sqrt{3}} & \frac{\sigma_{13} - i\sigma_{14}}{\sqrt{2}} \\ \frac{\sigma_9 + i\sigma_{10}}{\sqrt{2}} & \frac{\sigma_{11} + i\sigma_{12}}{\sqrt{2}} & \frac{\sigma_{13} + i\sigma_{14}}{\sqrt{2}} & \frac{\sigma_0}{2} - \frac{\sqrt{3}}{2}\sigma_{15} \end{pmatrix}. \tag{39}$$

In a similar manner, the pseudo-scalar mesons are given as

$$T_a \pi_a = \frac{1}{\sqrt{2}} \begin{pmatrix} \frac{\pi_0}{2} + \frac{\pi_3}{\sqrt{2}} + \frac{\pi_8}{\sqrt{6}} + \frac{\pi_{15}}{2\sqrt{3}} & \frac{\pi_1 - i\pi_2}{\sqrt{2}} & \frac{\pi_4 - i\pi_5}{\sqrt{2}} & \frac{\pi_9 - i\pi_{10}}{\sqrt{2}} \\ \frac{\pi_1 + i\pi_2}{\sqrt{2}} & \frac{\pi_0}{\sqrt{2}} - \frac{\pi_3}{\sqrt{2}} + \frac{\pi_8}{\sqrt{6}} + \frac{\pi_{15}}{2\sqrt{3}} & \frac{\pi_6 - i\pi_7}{\sqrt{2}} & \frac{\pi_{11} - i\pi_{12}}{\sqrt{2}} \\ \frac{\pi_4 + i\pi_5}{\sqrt{2}} & \frac{\pi_6 + i\pi_7}{\sqrt{2}} & \frac{\pi_0}{2} - \sqrt{\frac{2}{3}}\pi_8 + \frac{\pi_{15}}{2\sqrt{3}} & \frac{\pi_{13} - i\pi_{14}}{\sqrt{2}} \\ \frac{\pi_9 + i\pi_{10}}{\sqrt{2}} & \frac{\pi_{11} + i\pi_{12}}{\sqrt{2}} & \frac{\pi_{13} + i\pi_{14}}{\sqrt{2}} & \frac{\pi_0}{2} - \frac{\sqrt{3}}{2}\pi_{15} \end{pmatrix}. \tag{40}$$

It is apparent that the global minima, defined by the absence of partial derivatives related to σ_x , σ_y , and σ_c , give rise to

$$h_x = m^2\sigma_x - \frac{c}{2}\sigma_x\sigma_y\sigma_c + \ell_1\sigma_x\sigma_y^2 + \ell_2\sigma_x\sigma_c^2 + \frac{1}{2}(2\ell_1 + \ell_2)\sigma_x^2, \tag{41}$$

$$h_y = m^2\sigma_y - \frac{c}{2}\sigma_x^2\sigma_c + \ell_1\sigma_x^2\sigma_y + \ell_2\sigma_y\sigma_c^2 + (\ell_1 + \ell_2)\sigma_y^2, \tag{42}$$

$$h_c = m^2\sigma_c - \frac{c}{2}\sigma_x^2\sigma_y + \ell_1\sigma_x^2\sigma_c + \ell_2\sigma_y^2\sigma_c + (\ell_1 + \ell_2)\sigma_c^3, \tag{43}$$

When considering an external field Δ , represented by the Lagrangian term $\text{Tr}[\Delta(L^{\mu\nu} + L^{\mu\nu})]$, we arrived at the following result:

$$\Delta = \sum_{a=0}^{N_f^2-1} h_a\delta_a = h_0\delta_0 + h_8\delta_{15} + h_a\delta_{15}, \tag{44}$$

$$= \begin{pmatrix} \delta_u & 0 & 0 & 0 \\ 0 & \delta_d & 0 & 0 \\ 0 & 0 & \delta_s & 0 \\ 0 & 0 & 0 & \delta_c \end{pmatrix}, \tag{45}$$

from which we deduced that

$$\begin{pmatrix} \delta_u \\ \delta_d \\ \delta_s \\ \delta_c \end{pmatrix} = \begin{pmatrix} m_u^2 \\ m_d^2 \\ m_s^2 \\ m_c^2 \end{pmatrix}. \tag{46}$$

N_f gives the number of quark flavors.

Through the application of the electromagnetic field $A_\mu = gA_\mu^a\lambda^a/2$, we derived vector and axial vector meson nonets:

$$L^{\mu\nu} = \delta_\mu L^\nu - ieA^\mu[T_3, L^\nu] - \{\delta^\nu \mathcal{L}^\mu - ieA^\nu[T_3, L^\mu]\}, \tag{47}$$

$$R^{\mu\nu} = \delta_\mu R^\nu - ieA^\mu[T_3, R^\nu] - \{\delta^\nu R^\mu - ieA^\nu[T_3, R^\mu]\}, \tag{48}$$

where $L^\mu = \sum_{a=0}^{N_f^2-1} T_a(V_a^\mu + A_a^\mu)$ and $R^\mu = \sum_{a=0}^{N_f^2-1} T_a(V_a^\mu - A_a^\mu)$. The nonvanishing external field matrices H and ϵ clearly break chiral symmetry:

$$H = \sum_{a=0}^{N_f^2-1} h_a T_a = h_0 T_0 + h_8 T_8 + h_{15} T_{15}, \tag{49}$$

$$\epsilon = \epsilon_c = m_c^2 = \frac{1}{2} [m_{\chi_{c0}}^2 - m_0^2 - \ell_1(\sigma_x^2 + \sigma_y^2) - 3\sigma_c^2(\ell_1 + \ell_2)]. \tag{50}$$

Generators of the group $U(N_f)$ are $T_a = \lambda_a/2$, where λ_a are the Gell-Mann matrices.

In the isospin-symmetric approximation, it is possible to assign the values $\delta_u = \delta_d = 0$. Consequently, for the parameters δ_x , δ_y , and δ_c , one may utilize the mass equations of vector mesons, such as $m_{\omega_N}^2$, $m_{\omega_S}^2$, and $m_{\chi_{c1}}^2$. Then, we obtained

$$\delta_x = \frac{1}{2} \left[m_{\omega_N}^2 - m_1^2 + m_0^2 - \frac{\sigma_x^2}{2}(h_1 + h_2 + h_3) - \frac{h_1}{2}(\sigma_y^2 + \sigma_c^2) \right], \tag{51}$$

$$\delta_y = \frac{1}{2} \left[m_{\omega_S}^2 - m_1^2 + m_0^2 - \frac{\sigma_y^2}{2} \left(\frac{h_1}{2} + h_2 + h_3 \right) - \frac{h_1}{2}(\sigma_x^2 + \sigma_c^2) \right], \tag{52}$$

$$\delta_c = \frac{1}{2} \left[m_{\chi_{c1}}^2 - m_1^2 + m_0^2 - 2g_1^2\sigma_c^2 - \sigma_c^2 \left(\frac{h_1}{2} + h_2 - h_3 \right) - \frac{h_1}{2}(\sigma_y^2 + \sigma_y^2) \right]. \tag{53}$$

The other mass parameters are given as follows:

$$m^2 = m_\pi^2 - \frac{f_\pi^2}{2} \ell_2 + \mathcal{C} \left[f_K - \frac{f_\phi}{2} \right] - \ell_1 \left[f_K - \frac{f_\pi}{2} \right]^2, \tag{54}$$

$$m_0^2 = \frac{1}{2} \left[m_{a_0}^2 + m_{\sigma_s}^2 - \ell_2 \left(\frac{3}{2} \sigma_x^2 + 3\sigma_y^2 \right) \right]. \tag{55}$$

It is important to note that the parameters $h_1, h_2,$ and h_3 are connected to the quark condensates $\sigma_u, \sigma_d,$ and $\sigma_s,$ which can be formulated in relation to $\sigma_0, \sigma_3,$ and σ_8 :

$$\sigma_u = \sqrt{2}\sigma_0 + \sigma_3 + \sigma_8, \tag{56}$$

$$\sigma_d = \sqrt{2}\sigma_0 - \sigma_3 + \sigma_8, \tag{57}$$

$$\sigma_s = \sigma_0 - \sqrt{2}\sigma_8. \tag{58}$$

Accordingly, $h_0, h_3,$ and h_8 are specified as

$$h_0 = \frac{1}{\sqrt{6}} \left[f_\pi m_\pi^2 + 2f_K m_k^2 \right], \tag{59}$$

$$h_3 = \left[m^2 + \frac{\mathcal{C}}{\sqrt{6}} \sigma_0 - \frac{\mathcal{C}}{\sqrt{6}} \sigma_8 + \ell_1 \left(\sigma_0^2 + \sigma_3^2 + \sigma_8^2 \right) + \ell_2 \left(\sigma_0^2 + \frac{\sigma_3^2}{2} + \frac{\sigma_8^2}{2} + \sqrt{2}\sigma_0\sigma_8 \right) \right] \sigma_3, \tag{60}$$

$$h_8 = \frac{2}{3} \left[f_\pi m_\pi^2 - 2f_K m_k^2 \right]. \tag{61}$$

In the $SU(4)_\ell \times SU(4)_r$ model, the quark condensates are given as

$$\sigma_x = \frac{\sigma_0}{\sqrt{2}} + \frac{\sigma_8}{\sqrt{3}} + \frac{\sigma_{15}}{\sqrt{6}}, \tag{62}$$

$$\sigma_y = \frac{\sigma_0}{2} - \sqrt{\frac{2}{3}}\sigma_8 + \frac{1}{2\sqrt{3}}\sigma_{15}, \tag{63}$$

$$\sigma_c = \frac{\sigma_0}{2} - \frac{\sqrt{3}}{2}\sigma_{15}, \tag{64}$$

where σ_x refers to the condensate of light quarks, i.e., nondegenerate up and down quarks, whereas σ_y (σ_c) represents the strange (charm) quark condensate. The complex matrix of dimensions $N_f \times N_f$ is associated with the scalar $J^{PC} = 0^{++}$, pseudoscalar $J^{PC} = 0^{-+}$, vector $J^{PC} = 0^{--}$, and axial vector $J^{PC} = 0^{+-}$ mesons [50]. By applying the formula $m_0 = (g/2)\Phi$, where g represents the Yukawa coupling, it is possible to relate the quark masses to the quark condensates:

$$m_u = \frac{g}{2} \left[\frac{\sigma_0}{\sqrt{2}} + \frac{\sigma_8}{\sqrt{3}} + \frac{\sigma_{15}}{\sqrt{6}} \right] = \frac{g}{2} \sigma_x, \tag{65}$$

$$m_d = \frac{g}{2} \left[\frac{\sigma_0}{\sqrt{2}} + \frac{\sigma_8}{\sqrt{3}} + \frac{\sigma_{15}}{\sqrt{6}} \right] = \frac{g}{2} \sigma_x, \tag{66}$$

$$m_s = \frac{g}{2} \left[\frac{\sigma_0}{\sqrt{2}} - \frac{2\sigma_8}{\sqrt{3}} + \frac{\sigma_{15}}{\sqrt{6}} \right] = \frac{g}{\sqrt{2}} \sigma_y, \tag{67}$$

$$m_c = \frac{g}{2} \left[\frac{\sigma_0}{\sqrt{2}} - \sqrt{\frac{3}{2}}\sigma_{15} \right] = \frac{g}{\sqrt{2}} \sigma_c. \tag{68}$$

At finite temperature, $\sigma_x \rightarrow \sigma_x(T), \sigma_y \rightarrow \sigma_y(T),$ and $\sigma_c \rightarrow \sigma_c(T).$ Additionally, it is required that all eLSM parameters be formulated as functions of temperature. As elaborated in Section 2.1, the masses of different meson states can be obtained from the

second derivative of the grand potential with respect to their respective mass fields (11). For SU(4), $a, b \in [0, 1, \dots, 15]$. Below is a compilation of the masses associated with the noncharged meson states.

- Pseudoscalar charmed mesons:

$$m_{\pi}^2(T) = Z_{\pi}^2(T) \left[m_0^2 \left(1 + \frac{T^2}{T_0^2} \right) + \left(\ell_1(T) + \frac{\ell_2(T)}{2} \right) \sigma_x^2(T) + \ell_1(T) \sigma_y^2(T) + \ell_1(T) \sigma_c^2(T) \right], \tag{69}$$

$$m_K^2(T) = Z_K^2(T) \left[m_0^2 \left(1 + \frac{T^2}{T_0^2} \right) + \left(\ell_1(T) + \frac{\ell_2(T)}{2} \right) \sigma_x^2(T) - \frac{\ell_2(T)}{\sqrt{2}} \sigma_x(T) \sigma_y(T) + \ell_1(T) \left[\sigma_y^2(T) + \sigma_c^2(T) \right] + \ell_2(T) \sigma_y^2(T) \right], \tag{70}$$

$$m_{\eta_N}^2(T) = Z_{\eta_N}^2(T) \left[m_0^2 \left(1 + \frac{T^2}{T_0^2} \right) + \left(\ell_1(T) + \frac{\ell_2(T)}{2} \right) \sigma_x^2(T) + \ell_1(T) \left[\sigma_y^2(T) + \sigma_c^2(T) \right] + \frac{c}{2} \sigma_x^2(T) \sigma_y^2(T) \sigma_c^2(T) \right], \tag{71}$$

$$m_{\eta_S}^2(T) = Z_{\eta_S}^2(T) \left[m_0^2 \left(1 + \frac{T^2}{T_0^2} \right) + \ell_1(T) \left(\sigma_x^2(T) + \sigma_c^2(T) \right) + [\ell_1(T) + \ell_2(T)] \sigma_y^2(T) + \frac{C}{8} \sigma_x^2(T) \sigma_c^2(T) \right]. \tag{72}$$

- Scalar charmed mesons:

$$m_{a_0}^2(T) = m_0^2 \left(1 + \frac{T^2}{T_0^2} \right) + \ell_1(T) \left[\sigma_x^2(T) + \sigma_y^2(T) + \sigma_c^2(T) \right] + \frac{3\ell_2(T)}{2} \sigma_x^2(T), \tag{73}$$

$$m_{k_0^*}^2(T) = Z_{k_0^*}^2(T) \left[m_0^2 \left(1 + \frac{T^2}{T_0^2} \right) + \left[\ell_1(T) + \frac{\ell_2(T)}{2} \right] \sigma_x^2(T) + \frac{\ell_2(T)}{\sqrt{2}} \sigma_x(T) \sigma_y(T) + \ell_1(T) \left[\sigma_y^2(T) + \sigma_c^2(T) \right] + \ell_2(T) \sigma_y^2(T) \right], \tag{74}$$

$$m_{\sigma_N}^2(T) = m_0^2 \left(1 + \frac{T^2}{T_0^2} \right) + 3 \left[\ell_1(T) + \frac{\ell_2(T)}{2} \right] \sigma_x^2(T) + \ell_1(T) \left[\sigma_y^2(T) + \sigma_c^2(T) \right], \tag{75}$$

$$m_{\sigma_S}^2(T) = m_0^2 \left(1 + \frac{T^2}{T_0^2} \right) + \ell_1(T) \left[\sigma_x^2(T) + \sigma_c^2(T) \right] + 3[\ell_1(T) + \ell_2(T)] \sigma_y^2(T). \tag{76}$$

- Vector charmed mesons:

$$m_{\omega_N}^2(T) = m_1^2(T) - m_0^2 \frac{T^2}{T_0^2} + \frac{1}{2} [h_1(T) + h_2(T) + h_3(T)] \sigma_x^2(T) + \frac{h_1(T)}{2} \left[\sigma_y^2(T) + \sigma_c^2(T) \right] + 2\delta_x(T), \tag{77}$$

$$m_{\omega_S}^2(T) = m_1^2(T) - m_0^2 \frac{T^2}{T_0^2} + \frac{h_1(T)}{2} \left[\sigma_x^2(T) + \sigma_c^2(T) \right] + \left[\frac{h_1(T)}{2} + h_2(T) + h_3(T) \right] \sigma_y^2(T) + 2\delta_x(T), \tag{78}$$

$$m_{K^*}^2(T) = m_1^2(T) - m_0^2 \frac{T^2}{T_0^2} + \frac{\sigma_x^2(T)}{4} \left[g_1^2(T) + 2h_1(T) + h_2(T) \right] + \frac{\sigma_x(T)}{\sqrt{2}} \sigma_x(T) \sigma_y(T) \left[h_3(T) - g_1^2(T) \right] + \frac{\sigma_y^2(T)}{2} \left[g_1^2(T) + h_1(T) + h_2(T) \right] + h_1(T) \frac{\sigma_c^2(T)}{2} + \delta_x(T) + \delta_y(T), \tag{79}$$

$$m_{\rho}^2(T) = m_{\omega_N}^2(T). \tag{80}$$

- Axial vector charmed mesons:

$$m_{a_1}^2(T) = m_1^2(T) - m_0^2 \frac{T^2}{T_0^2} + \frac{h_1(T)}{2} [\sigma_y^2(T) + \sigma_c^2(T)] + \frac{\sigma_x^2(T)}{2} [h_1(T) + h_2(T) - h_3(T)] + 2\delta_x(T), \tag{81}$$

$$m_{f_{1s}}^2(T) = m_1^2(T) - m_0^2 \frac{T^2}{T_0^2} + \frac{h_1(T)}{2} [\sigma_x^2(T) + \sigma_c^2(T)] + \left[\frac{h_1(T)}{2} + h_2(T) - h_3(T) \right] \sigma_y^2(T) + 2\delta_y(T), \tag{82}$$

$$m_{k_1}^2(T) = m_1^2(T) - m_0^2 \frac{T^2}{T_0^2} + \frac{1}{4} \sigma_x^2(T) [g_1^2(T) + 2h_1(T) + h_2(T)] + \frac{\sigma_y^2(T)}{2} [g_1^2(T) + h_1(T) + h_2(T)] - \frac{1}{\sqrt{2}} \sigma_x(T) \sigma_y(T) [g_1^2(T) - h_3(T)] + \frac{h_1(T)}{2} \sigma_c^2(T) + \delta_x(T) + \delta_y(T), \tag{83}$$

$$m_{1N}^2(T) = m_{a_1}^2(T). \tag{84}$$

These sixteen meson states can be systematically analyzed in relation to the non-charmed meson states outlined in Section 2.1. We now introduce the analytical expressions that describe the masses associated with charmed meson states.

- Pseudoscalar charmed mesons:

$$m_D^2(T) = Z_D^2(T) \left[m_0^2 \left(1 + \frac{T^2}{T_0^2} \right) + \left(\ell_1(T) + \frac{\ell_2(T)}{2} \right) \sigma_x^2(T) + \ell_1(T) \sigma_y^2(T) + [\ell_1(T) + \ell_2(T)] \sigma_c^2(T) - \frac{\ell_2(T)}{\sqrt{2}} \sigma_x(T) \sigma_c(T) + \epsilon_c(T) \right], \tag{85}$$

$$m_{\eta_c}^2(T) = Z_{\eta_c}^2(T) \left[m_0^2 \left(1 + \frac{T^2}{T_0^2} \right) + \lambda_1 [\sigma_x^2(T) + \sigma_y^2(T)] + (\ell_1(T) + \ell(T)_2) \sigma_c^2(T) + \frac{c}{8} \sigma_x^2(T) \sigma_y^2(T) + 2\epsilon_c(T) \right], \tag{86}$$

$$m_{D_s}^2(T) = Z_{D_s}^2 \left[m_0^2 \left(1 + \frac{T^2}{T_0^2} \right) + \ell_1(T) \sigma_x^2(T) + [\ell_1(T) + \ell_2(T)] \sigma_y^2(T) + [\ell_1(T) + \ell_2(T)] \sigma_c^2(T) - \ell_2(T) \sigma_y(T) \sigma_c(T) + \epsilon_c(T) \right]. \tag{87}$$

- Scalar charmed mesons:

$$m_{\chi_{c0}}^2(T) = m_0^2 \left(1 + \frac{T^2}{T_0^2} \right) + \ell_1(T) [\sigma_x^2(T) + \sigma_y^2(T)] + 3[\ell_1(T) + \ell_2(T)] \sigma_c^2(T) + 2\epsilon_c(T), \tag{88}$$

$$m_{D_0^*}^2(T) = Z_{D_0^*}^2 \left[m_0^2 \left(1 + \frac{T^2}{T_0^2} \right) + \left(\ell_1(T) + \frac{\ell_2(T)}{2} \right) \sigma_x^2(T) + \ell_1(T) \sigma_y^2(T) + \frac{\ell_2(T)}{\sqrt{2}} \sigma_x(T) \sigma_c(T) + [\ell_1(T) + \ell_2(T)] \sigma_c^2(T) + \epsilon_c(T) \right], \tag{89}$$

$$m_{D_0^{*0}}^2(T) = Z_{D_0^{*0}}^2 \left[m_0^2 \left(1 + \frac{T^2}{T_0^2} \right) + \left(\ell_1(T) + \frac{\ell_2(T)}{2} \right) \sigma_x^2(T) + \ell_1(T) \sigma_y^2(T) + \frac{\ell_2(T)}{\sqrt{2}} \sigma_x(T) \sigma_c(T) + [\ell_1(T) + \ell_2(T)] \sigma_c^2(T) + \epsilon_c(T) \right], \tag{90}$$

$$m_{D_{s0}^*}^2(T) = Z_{D_{s0}^*}^2 \left[m_0^2 \left(1 + \frac{T^2}{T_0^2} \right) + \ell_1(T) \sigma_x^2(T) + [\ell_1(T) + \ell_2(T)] \sigma_y^2(T) + \ell_2(T) \sigma_y(T) \sigma_c(T) + [\ell_1(T) + \ell_2(T)] \sigma_c^2(T) + \epsilon_c(T) \right]. \tag{91}$$

- Vector charmed mesons:

$$\begin{aligned}
 m_{D^*}^2(T) &= m_1^2(T) - m_0^2 \frac{T^2}{T_0^2} + \left(\frac{g_1^2(T)}{2} + h_1(T) + \frac{h_2(T)}{2} \right) \frac{\sigma_x^2(T)}{2} \\
 &\quad + \frac{1}{\sqrt{2}} \sigma_x(T) \sigma_c(T) [h_3(T) - g_1^2(T)] + \frac{1}{2} (g_1^2(T) + h_1(T) + h_2(T)) \sigma_c^2(T) \\
 &\quad + h_1(T) \frac{\sigma_y^2(T)}{2} + \delta_x(T) + \delta_c(T), \tag{92}
 \end{aligned}$$

$$\begin{aligned}
 m_{J/\psi}^2(T) &= m_1^2(T) - m_0^2 \frac{T^2}{T_0^2} + \frac{h_1(T)}{2} [\sigma_x^2(T) + \sigma_y^2(T)] \\
 &\quad + \left(\frac{h_1(T)}{2} + h_2(T) + h_3(T) \right) \sigma_c^2(T) + 2\delta_c(T), \tag{93}
 \end{aligned}$$

$$\begin{aligned}
 m_{D_s^*}^2(T) &= m_1^2(T) - m_0^2 \frac{T^2}{T_0^2} + \frac{1}{2} (g_1^2(T) + h_1(T) + h_2(T)) [\sigma_y^2(T) + \sigma_c^2(T)] \\
 &\quad + \frac{h_1(T)}{2} \sigma_x^2(T) + (h_3(T) - g_1^2(T)) \sigma_y(T) \sigma_c(T) + \delta_y(T) + \delta_c(T). \tag{94}
 \end{aligned}$$

- Axial vector charmed mesons:

$$\begin{aligned}
 m_{D_{s1}}^2(T) &= m_1^2(T) - m_0^2 \frac{T^2}{T_0^2} + \frac{1}{2} (g_1^2(T) + h_1(T) + h_2(T)) [\sigma_y^2(T) - \sigma_c^2(T)] \\
 &\quad - \sigma_y(T) \sigma_c(T) (g_1^2(T) + h_3(T)) + \frac{h_1(T)}{2} \sigma_x^2(T) + \delta_y(T) + \delta_c(T), \tag{95}
 \end{aligned}$$

$$\begin{aligned}
 m_{D_1}^2(T) &= m_1^2(T) - m_0^2 \frac{T^2}{T_0^2} + \frac{1}{4} (g_1^2(T) + 2h_1(T) + h_2(T)) \sigma_x^2(T) \\
 &\quad + \frac{1}{2} (g_1^2(T) + h_1(T) + h_2(T)) \sigma_c^2(T) - \frac{1}{\sqrt{2}} (g_1^2(T) + h_3(T)) \sigma_x(T) \sigma_c(T) \\
 &\quad + h_1(T) \frac{\sigma_y^2(T)}{2} + \delta_x(T) + \delta_c(T), \tag{96}
 \end{aligned}$$

$$\begin{aligned}
 m_{\chi_{c1}}^2(T) &= m_1^2(T) - m_0^2 \frac{T^2}{T_0^2} + \frac{h_1(T)}{2} [\sigma_x^2(T) + \sigma_y^2(T)] \\
 &\quad + \left[\frac{h_1(T)}{2} + h_2(T) - h_3(T) \right] \sigma_c^2(T) + 2\delta_c(T). \tag{97}
 \end{aligned}$$

The wavefunction renormalization factors found in the previous expressions are given as follows:

$$Z_{K_s}(T) = \frac{2m_K(T)}{\sqrt{4m_K^2(T) - g_1^2(T) [\sigma_x(T) + \sqrt{2}\sigma_y(T)]^2}}, \tag{98}$$

$$Z_{\eta_c}(T) = \frac{m_{\chi_{c1}}(T)}{\sqrt{m_{\chi_{c1}}^2(T) - 2g_1^2(T)\sigma_c^2(T)}}, \tag{99}$$

$$Z_D(T) = \frac{2m_{D_1}(T)}{\sqrt{4m_{D_1}^2(T) - g_1^2(T) [\sigma_c(T) + \sqrt{2}\sigma_c(T)]^2}}, \tag{100}$$

$$Z_{D_s}(T) = \frac{\sqrt{2}m_{D_{s1}}(T)}{\sqrt{2m_{D_{s1}}^2(T) - g_1^2(T) [\sigma_y^2(T) + \sigma_c(T)]^2}}, \tag{101}$$

$$Z_{D_0^*}(T) = \frac{2m_{D^*}(T)}{\sqrt{4m_{D^*}^2(T) - g_1^2(T) [\sigma_x^2(T) - \sqrt{2}\sigma_c(T)]^2}}, \tag{102}$$

$$Z_{D_0^{*0}}(T) = \frac{2m_{D^{*0}}(T)}{\sqrt{4m_{D^{*0}}^2(T) - g_1^2(T) [\sigma_x(T) - \sqrt{2}\sigma_c(T)]^2}}, \tag{103}$$

$$Z_{D_{s0}^*}(T) = \frac{\sqrt{2}m_{D_s^*}(T)}{\sqrt{2m_{D_s^*}^2(T) - g_1^2(T) [\sigma_y(T) - \sigma_c(T)]^2}}. \tag{104}$$

The section that follows is devoted to the final conclusions and outlook.

3. Conclusions and Outlook

Through the incorporation of mesonic contributions within the eLSM potential, considering both three and four quark flavors, we introduce an analytical methodology for the evaluation of the masses associated with diverse meson states. We derived meson states expressed as $\langle \bar{q}q \rangle = \langle \bar{q}_\ell q_r - \bar{q}_\ell q_r \rangle \neq 0$ from the effective Lagrangian of the extended linear sigma model, considering scenarios both with and without charm quarks. In terms of their quantum numbers, including the orbital angular momentum J , parity P , and charge conjugation C , these meson states could be classified into several categories: pseudoscalar states with quantum numbers $J^{PC} = 0^{-+}$, scalar states with $J^{PC} = 0^{++}$, vector states with $J^{PC} = 1^{--}$, and axial vector states with $J^{PC} = 1^{+-}$. We introduce analytical expressions for the mass spectrum of seventeen noncharmed and twenty-nine charmed meson states at finite temperature.

The present analytical analyses serve to establish a groundwork for the modification of meson masses in a thermal medium. This investigation was dedicated to the thermal environment and considered the dependence of forty-six mesons, both with and without charm quarks, on finite temperature. As a future direction, we aim to assess the temperature dependence of meson masses through numerical methods. Furthermore, the impact of a finite chemical potential on these meson states could be the subject of subsequent research.

Author Contributions: Conceptualization, A.N.T.; Methodology, A.N.T. and A.F.; Validation, M.H.; Formal analysis, A.N.T., A.I.A., A.F. and Y.K.; Investigation, A.N.T., A.I.A. and A.F.; Writing—original draft, A.N.T.; Writing—review & editing, A.F., Y.K., A.A. and M.H.; Project administration, A.A. All authors read and agreed to the published version of this manuscript.

Funding: This research received no external funding.

Data Availability Statement: The authors confirm that the data supporting the findings of this study are available within this article.

Acknowledgments: The authors would like to recognize the support offered by the Egyptian Academy for Scientific Research and Technology (ASRT) provided through the ASRT/JINR joint projects (Call 2023), which made it possible to conduct this research at the Joint Institute for Nuclear Research (JINR) in the Russian Federation.

Conflicts of Interest: The authors declare no conflicts of interest.

Appendix A. Amendments to [50]

The publication [50] was released in the MDPI *Particles* journal. It includes a number of printing mistakes. Here is a summary of corrections:

Equation (16) $\rightarrow \frac{\sigma_0}{2} - \frac{\sqrt{3}}{s}\sigma_{15},$

Equation (30) $\rightarrow Z_K^2 \left[m_0^2 + \left(\lambda_1 + \frac{\lambda_2}{2} \right) \sigma_x^2 - \frac{\lambda_2}{\sqrt{2}} \sigma_x \sigma_y + \lambda_1 (\sigma_y^2 + \sigma_c^2) + \lambda_2 \sigma_y^2 \right],$

Equation (34) $\rightarrow Z_{K^*}^2 \left[m_0^2 + \left(\lambda_1 + \frac{\lambda_2}{2} \right) \sigma_x^2 + \frac{\lambda_2}{\sqrt{2}} \sigma_x \sigma_y + \lambda_1 (\sigma_y^2 + \sigma_c^2) + \lambda_2 \sigma_y^2 \right],$

Equation (41) $\rightarrow m_1^2 - m_0^2 + \cancel{\frac{2g_1^2 \sigma_x^2}{81}} + \frac{1}{2} h_1 [\sigma_y^2 + \sigma_c^2] + \frac{1}{2} \sigma_x^2 [h_1 + h_2 + h_3] + 2\delta_x,$

Equation (42) $\rightarrow m_1^2 - m_0^2 + \frac{1}{2} h_1 [\sigma_x^2 + \sigma_c^2] + \cancel{\frac{2g_1^2 \sigma_c^2}{81}} + \frac{1}{2} [h_1 + 2h_2 - 2h_3] \sigma_y^2 + 2\delta_y,$

Equation (43) $\rightarrow m_1^2 - m_0^2 + \frac{1}{4} \sigma_x^2 (g_1^2 + 2h_1 + h_2) + \frac{1}{2} \sigma_y^2 (g_1^2 + h_1 + h_2) - \frac{1}{\sqrt{2}} \sigma_x \sigma_y (g_1^2 + h_3) + \frac{1}{2} h_1 \sigma_c^2 + \delta_x + \sigma_y,$

Equation (45) $\rightarrow Z_D^2 \left[m_0^2 + \left(\lambda_1 + \frac{\lambda_2}{2} \right) \sigma_x^2 + \lambda_1 \sigma_y^2 + (\lambda_1 + \lambda_2) \sigma_c^2 - \frac{\lambda_2}{2} \sigma_x \sigma_c + \epsilon_c \right],$

Equation (52) $\rightarrow m_1^2 - m_0^2 + \frac{1}{4} (g_1^2 + 2h_1 + h_2) \sigma_x^2 + \frac{1}{\sqrt{2}} \sigma_x \sigma_c (h_3 - g_1^2) + \frac{1}{2} (g_1^2 + h_1 + h_2) \sigma_c^2 + \frac{1}{2} h_1 \sigma_y^2 + \delta_x + \delta_c,$

Equation (55) $\rightarrow m_1^2 - m_0^2 + \frac{1}{2} (g_1^2 + h_1 + h_2) (\sigma_y^2 + \sigma_c^2) - \sigma_y \sigma_c (h_3 + g_1^2) + \frac{1}{2} h_1 \sigma_x^2 + \delta_y + \delta_c,$

Equation (56) $\rightarrow m_1^2 - m_0^2 + \frac{1}{4} (g_1^2 + 2h_1 + h_2) \sigma_x^2 + \frac{1}{2} (g_1^2 + h_1 + h_2) \sigma_c^2 - \frac{1}{\sqrt{2}} \sigma_x \sigma_c (h_3 + g_1^2) + \frac{1}{2} h_1 \sigma_y^2 + \delta_y + \delta_c,$

Equation (57) $\rightarrow m_1^2 - m_0^2 + \frac{1}{2} h_1 [\sigma_x^2 + \sigma_y^2] + \cancel{\frac{2g_1^2 \sigma_c^2}{81}} + \frac{1}{2} (h_1 + 2h_2 - 2h_3) \sigma_c^2 + 2\delta_c.$

References

1. Ferreira, M.N.; Papavassiliou, J. Gauge Sector Dynamics in QCD. *Particles* **2023**, *6*, 312–363. [\[CrossRef\]](#)
2. Gorenstein, M.I.; Mogilevsky, O.A. On a Nonperturbative Pressure Effect in Lattice QCD. *Z. Phys. C* **1988**, *38*, 161–163. [\[CrossRef\]](#)
3. Danzer, J.; Gattringer, C.; Liptak, L.; Marinkovic, M. A Study of the sign problem for lattice QCD with chemical potential. *Phys. Lett. B* **2009**, *682*, 240–245. [\[CrossRef\]](#)
4. Radzhabov, A.E.; Blaschke, D.; Buballa, M.; Volkov, M.K. Nonlocal PNJL model beyond mean field and the QCD phase transition. *Phys. Rev. D* **2011**, *83*, 116004. [\[CrossRef\]](#)
5. Contrera, G.A.; Grunfeld, A.G.; Blaschke, D.B. Phase diagrams in nonlocal Polyakov-Nambu-Jona-Lasinio models constrained by lattice QCD results. *Phys. Part. Nucl. Lett.* **2014**, *11*, 342–351. [\[CrossRef\]](#)
6. Karsch, F.; Redlich, K.; Tawfik, A. Hadron resonance mass spectrum and lattice QCD thermodynamics. *Eur. Phys. J. C* **2003**, *29*, 549–556. [\[CrossRef\]](#)
7. Karsch, F.; Redlich, K.; Tawfik, A. Thermodynamics at nonzero baryon number density: A Comparison of lattice and hadron resonance gas model calculations. *Phys. Lett. B* **2003**, *571*, 67–74. [\[CrossRef\]](#)
8. Tawfik, A. The Influence of strange quarks on QCD phase diagram and chemical freeze-out: Results from the hadron resonance gas model. *J. Phys. G* **2005**, *31*, S1105–S1110. [\[CrossRef\]](#)
9. Tawfik, A. QCD phase diagram: A Comparison of lattice and hadron resonance gas model calculations. *Phys. Rev. D* **2005**, *71*, 054502. [\[CrossRef\]](#)
10. Coppola, M.; Gómez Dumm, D.; Scoccola, N.N. Charged pion masses under strong magnetic fields in the NJL model. *Phys. Lett. B* **2018**, *782*, 155–161. [\[CrossRef\]](#)
11. Carlomagno, J.P.; Gomez Dumm, D.; Noguera, S.; Scoccola, N.N. Neutral pseudoscalar and vector meson masses under strong magnetic fields in an extended NJL model: Mixing effects. *Phys. Rev. D* **2022**, *106*, 074002. [\[CrossRef\]](#)

12. Carlomagno, J.P.; Gomez Dumm, D.; Villafañe, M.F.I.; Noguera, S.; Scoccola, N.N. Charged pseudoscalar and vector meson masses in strong magnetic fields in an extended NJL model. *Phys. Rev. D* **2022**, *106*, 094035. [[CrossRef](#)]
13. Nambu, Y.; Jona-Lasinio, G. Dynamical Model of Elementary Particles Based on an Analogy with Superconductivity. I. *Phys. Rev.* **1961**, *122*, 345–358. [[CrossRef](#)]
14. Gausterer, H.; Sanielevici, S. Can the Chiral Transition in QCD Be Described by a Linear σ Model in Three-dimensions? *Phys. Lett. B* **1988**, *209*, 533–537. [[CrossRef](#)]
15. Friesen, A.V.; Kalinovsky, Y.L.; Toneev, V.D. Strange matter and kaon to pion ratio in the SU(3) Polyakov–Nambu–Jona-Lasinio model. *Phys. Rev. C* **2019**, *99*, 045201. [[CrossRef](#)]
16. Kalinovsky, Y.L.; Friesen, A.V. Properties of mesons and critical points in the Nambu–Jona-Lasinio model with different regularizations. *Phys. Part. Nucl. Lett.* **2015**, *12*, 737–743. [[CrossRef](#)]
17. Friesen, A.V.; Kalinovsky, Y.L.; Toneev, V.D. Effects of Model Parameters in Thermodynamics of the PNJL Model. *Int. J. Mod. Phys. A* **2012**, *27*, 1250013. [[CrossRef](#)]
18. Giacosa, F.; Parganlija, D.; Kovacs, P.; Wolf, G. Phenomenology of light mesons within a chiral approach. *Eur. Phys. J. Web Conf.* **2012**, *37*, 08006. [[CrossRef](#)]
19. Tawfik, A.N.; Diab, A.M.; Ghoneim, M.T.; Anwer, H. SU(3) Polyakov Linear-Sigma Model With Finite Isospin Asymmetry: QCD Phase Diagram. *Int. J. Mod. Phys. A* **2019**, *34*, 1950199. [[CrossRef](#)]
20. Tawfik, A.N. QCD Phase Structure and In-Medium Modifications of Meson Masses in Polyakov Linear-Sigma Model with Finite Isospin Asymmetry. *Universe* **2023**, *9*, 276. [[CrossRef](#)]
21. Tawfik, A.N. Isospin Symmetry Breaking in Non-Perturbative QCD. *Phys. Sci. Forum* **2023**, *7*, 22. [[CrossRef](#)]
22. Tawfik, A.N.; Magdy, N. On SU(3) effective models and chiral phase-transition. *Adv. High Energy Phys.* **2015**, *2015*, 563428. [[CrossRef](#)]
23. Tawfik, A.N.; Magdy, N. SU(3) Polyakov linear- σ model in magnetic fields: Thermodynamics, higher-order moments, chiral phase structure, and meson masses. *Phys. Rev. C* **2015**, *91*, 015206. [[CrossRef](#)]
24. Eshraim, W.I.; Giacosa, F.; Rischke, D.H. Phenomenology of charmed mesons in the extended Linear Sigma Model. *Eur. Phys. J. A* **2015**, *51*, 112. [[CrossRef](#)]
25. Eshraim, W.I.; Fischer, C.S.; Giacosa, F.; Parganlija, D. Hybrid phenomenology in a chiral approach. *Eur. Phys. J. Plus* **2020**, *135*, 945. [[CrossRef](#)]
26. Gell-Mann, M.; Levy, M. The axial vector current in beta decay. *Nuovo Cim.* **1960**, *16*, 705. [[CrossRef](#)]
27. Burkert, V.D.; Elouadrhiri, L.; Afanasev, A.; Arrington, J.; Contalbrigo, M.; Cosyn, W.; Deshpande, A.; Glazier, D.I.; Ji, X.; Liuti, S.; et al. Precision studies of QCD in the low energy domain of the EIC. *Prog. Part. Nucl. Phys.* **2023**, *131*, 104032. [[CrossRef](#)]
28. Lenaghan, J.T.; Rischke, D.H. The O(N) model at finite temperature: Renormalization of the gap equations in Hartree and large N approximation. *J. Phys. G* **2000**, *26*, 431–450. [[CrossRef](#)]
29. Petropoulos, N. Linear sigma model and chiral symmetry at finite temperature. *J. Phys. G* **1999**, *25*, 2225–2241. [[CrossRef](#)]
30. Hu, B. Chiral SU(4) and scale invariance. *Phys. Rev. D* **1974**, *9*, 1825–1834. [[CrossRef](#)]
31. Schechter, J.; Singer, M. SU(4) sigma model. *Phys. Rev. D* **1975**, *12*, 2781–2790. [[CrossRef](#)]
32. Geddes, H.B. Spin-zero mass spectrum in the one-loop approximation in a linear SU(4) sigma model. *Phys. Rev. D* **1980**, *21*, 278–289. [[CrossRef](#)]
33. Ding, M.; Roberts, C.D.; Schmidt, S.M. Emergence of Hadron Mass and Structure. *Particles* **2023**, *6*, 57–120. [[CrossRef](#)]
34. Diab, A.M.; Ahmadov, A.I.; Tawfik, A.N.; Dahab, E.A.E. SU(4) Polyakov linear-sigma model at finite temperature and density. *Proc. Sci.* **2016**, *282*, 634. [[CrossRef](#)]
35. Abdel Aal Diab, A.M.; Tawfik, A.N. Quark-hadron phase structure of QCD matter from SU(4) Polyakov linear sigma model. *EPJ Web Conf.* **2018**, *177*, 09005. [[CrossRef](#)]
36. Tawfik, A.; Magdy, N.; Diab, A. Polyakov linear SU(3) σ model: Features of higher-order moments in a dense and thermal hadronic medium. *Phys. Rev. C* **2014**, *89*, 055210. [[CrossRef](#)]
37. Tawfik, A.N.; Diab, A.M. Polyakov SU(3) extended linear- σ model: Sixteen mesonic states in chiral phase structure. *Phys. Rev. C* **2015**, *91*, 015204. [[CrossRef](#)]
38. Tawfik, A.N.; Diab, A.M.; Ezzelarab, N.; Shalaby, A.G. QCD thermodynamics and magnetization in nonzero magnetic field. *Adv. High Energy Phys.* **2016**, *2016*, 1381479. [[CrossRef](#)]
39. Tawfik, A.N.; Diab, A.M.; Hussein, M.T. Quark–hadron phase structure, thermodynamics, and magnetization of QCD matter. *J. Phys. G* **2018**, *45*, 055008. [[CrossRef](#)]
40. Tawfik, A.N.; Diab, A.M.; Hussein, T.M. SU(3) Polyakov linear-sigma model: Bulk and shear viscosity of QCD matter in finite magnetic field. *Int. J. Adv. Res. Phys. Sci.* **2016**, *3*, 4–14.
41. Tawfik, A.N.; Diab, A.M.; Hussein, M.T. SU(3) Polyakov linear-sigma model: Conductivity and viscous properties of QCD matter in thermal medium. *Int. J. Mod. Phys. A* **2016**, *31*, 1650175. [[CrossRef](#)]

42. Tawfik, A.N.; Diab, A.M.; Hussein, M.T. SU(3) Polyakov linear-sigma model: Magnetic properties of QCD matter in thermal and dense medium. *J. Exp. Theor. Phys.* **2018**, *126*, 620–632. [[CrossRef](#)]
43. Tawfik, A.N.; Diab, A.M.; Hussein, M.T. Chiral phase structure of the sixteen meson states in the SU(3) Polyakov linear-sigma model for finite temperature and chemical potential in a strong magnetic field. *Chin. Phys. C* **2019**, *43*, 034103. [[CrossRef](#)]
44. Tawfik, A.N.; Greiner, C.; Diab, A.M.; Ghoneim, M.T.; Anwer, H. Polyakov linear- σ model in mean-field approximation and optimized perturbation theory. *Phys. Rev. C* **2020**, *101*, 035210. [[CrossRef](#)]
45. Tawfik, A.N.; Diab, A.M. Chiral magnetic properties of QCD phase-diagram. *Eur. Phys. J. A* **2021**, *57*, 200. [[CrossRef](#)]
46. Klempt, E.; Zaitsev, A. Glueballs, Hybrids, Multiquarks. Experimental facts versus QCD inspired concepts. *Phys. Rep.* **2007**, *454*, 1–202. [[CrossRef](#)]
47. Amsler, C.; Törnqvist, N.A. Mesons beyond the naive quark model. *Phys. Rep.* **2004**, *389*, 61–117. [[CrossRef](#)]
48. Vafa, C.; Witten, E. Restrictions on symmetry breaking in vector-like gauge theories. *Nucl. Phys. B* **1984**, *234*, 173–188. [[CrossRef](#)]
49. Rosenzweig, C.; Salomone, A.; Schechter, J. A Pseudoscalar Glueball, the Axial Anomaly and the Mixing Problem for Pseudoscalar Mesons. *Phys. Rev. D* **1981**, *24*, 2545–2548. [[CrossRef](#)]
50. Ahmadov, A.I.; Alshehri, A.A.; Tawfik, A.N. Mass Spectrum of Non-Charmed and Charmed Meson States in Extended Linear-Sigma Model. *Particles* **2024**, *7*, 560–575. [[CrossRef](#)]
51. Bowman, E.S.; Kapusta, J.I. Critical Points in the Linear Sigma Model with Quarks. *Phys. Rev. C* **2009**, *79*, 015202. [[CrossRef](#)]
52. Datta, S.; Gupta, S. Scaling and the continuum limit of the finite temperature deconfinement transition in SU(N_c) pure gauge theory. *Phys. Rev. D* **2009**, *80*, 114504. [[CrossRef](#)]
53. Particle Data Group; Zyla, P.; Barnett, R.M.; Beringer, J.; Dahl, O.; Dwyer, D.A.; Groom, D.E.; Lin, C.J.; Lugovsky, K.S.; Pianori, E.; et al. Review of Particle Physics. *Prog. Theor. Exp. Phys.* **2022**, *2022*, 083C01. [[CrossRef](#)]
54. Gasser, J.; Zarnauskas, G.R.S. On the pion decay constant. *Phys. Lett. B* **2010**, *693*, 122–128. [[CrossRef](#)]
55. Sanz-Cillero, J.J. Pion and kaon decay constants: Lattice versus resonance chiral theory. *Phys. Rev. D* **2004**, *70*, 094033. [[CrossRef](#)]
56. Schaefer, B.J.; Wagner, M. The Three-flavor chiral phase structure in hot and dense QCD matter. *Phys. Rev. D* **2009**, *79*, 014018. [[CrossRef](#)]
57. Schaefer, B.J.; Wambach, J. Susceptibilities near the QCD (tri)critical point. *Phys. Rev. D* **2007**, *75*, 085015. [[CrossRef](#)]
58. Scavenius, O.; Mocsy, A.; Mishustin, I.N.; Rischke, D.H. Chiral phase transition within effective models with constituent quarks. *Phys. Rev. C* **2001**, *64*, 045202. [[CrossRef](#)]
59. Cheng, M.; Christ, N.H.; Datta, S.; Van der Heide, J.; Jung, C.; Karsch, F.; Kaczmarek, O.; Laermann, E.; Mawhinney, R.D.; Miao, C.; et al. The QCD equation of state with almost physical quark masses. *Phys. Rev. D* **2008**, *77*, 014511. [[CrossRef](#)]
60. Kapusta, J.I.; Gale, C. *Finite-Temperature Field Theory: Principles and Applications*; Cambridge Monographs on Mathematical Physics, Cambridge University Press: Cambridge, UK, 2011. [[CrossRef](#)]
61. Parganlija, D.; Kovacs, P.; Wolf, G.; Giacosa, F.; Rischke, D.H. Meson vacuum phenomenology in a three-flavor linear sigma model with (axial-)vector mesons. *Phys. Rev. D* **2013**, *87*, 014011. [[CrossRef](#)]

Disclaimer/Publisher’s Note: The statements, opinions and data contained in all publications are solely those of the individual author(s) and contributor(s) and not of MDPI and/or the editor(s). MDPI and/or the editor(s) disclaim responsibility for any injury to people or property resulting from any ideas, methods, instructions or products referred to in the content.